$Al_{24.2}Si_{3.25}Cu_{24.2}Ni_{24.2}Ti_{24.2}$ high-entropy intermetallic alloy: Effect of nitrogen environment sintered microstructure and mechanical properties

Syed Fida Hassan[1,2]*, Ghaith Jamal Nadhreen[1]

[1] *Department of Mechanical Engineering, King Fahd University of Petroleum and Minerals, Dhahran 31261, Saudi Arabia*
[2] *Interdisciplinary Research Center for Advanced Materials, King Fahd University of Petroleum and Minerals, Dhahran 31261, Saudi Arabia*

Abstract

In this study, a lightweight $Al_{24.2}Si_{3.25}Cu_{24.2}Ni_{24.2}Ti_{24.2}$ high-entropy alloy was developed by sonication blending of the pure elements followed by the high-temperature sintering in the nitrogen gas environment. Microstructural characterization of the sintered alloy showed a fair dispersion of the elemental particles in the matrix during the blending process and the absorption of nitrogen, which led to the formation of multiple intermetallic compounds, including the nitrides, during the sintering process. Mechanical characterization of the sintered alloy revealed significantly high microhardness values with relatively lower compressive strength in $Al_{24.2}Si_{3.25}Cu_{24.2}Ni_{24.2}Ti_{24.2}$ alloy.

K e y w o r d s: high-entropy alloy, powder metallurgy, nitrogen, mechanical property

1. Introduction

Structural materials require a wide range of characteristics, like high strength, reasonably good ductility, higher toughness, thermal stability, and resistance to mechanical and/or environmental degradation. However, the limitation in manipulating composition and the ensued microstructure in traditional single-principle elemental alloys is the primary constraint to pushing the boundary of these properties in them. A very non-traditional approach was proposed barely more than a decade ago [1, 2], where the single-principle element role is replaced by multi-principle elements to push the boundaries of these structural properties. These multi-principle elemental alloys displayed the potential of unique microstructural features with an extraordinary level of physical and mechanical properties and hence garnered immense attention for further exploration [1–10]. The materials designed in this approach typically contain five or more principal elements in equiatomic proportion and are commonly known as high-entropy alloys (HEA). Baseless

alloy, concentrated solid solution alloy, compositionally complex alloy, and multi-principle element alloy are the few commonly used synonyms for this high-entropy alloy. As indicated by the name, the high-entropy alloys are especially metallic and dominate by transitional and refractory materials followed by lightweight materials [5, 11, 12], with some exceptions to explore non-metallic materials [13]. The design of these alloys typically involves mixing in a proportion that produces higher entropy in the solid solution, induces severe lattice distortion, and prompts non-equilibrium sluggish solid-state diffusion and a powerful cocktail effect [3, 11, 14, 15]. The complex and/or concentrated phases developed in the high-entropy alloys naturally experience severe lattice distortion due to the atomic size differences of the constituent elements present in higher amounts, which is more intense than the lattice distortion in traditional single--principle element alloys. The severe lattice distortion induces excessive configurational entropy in the high--entropy alloy due to the higher uncertainty in atomic lattice position. The effect becomes evident in the re-

*Corresponding author: tel.: +966 13 860 7787; e-mail addresses: sfhassan@kfupm.edu.sa, itsforfida@gmail.com

duced X-ray peak during the phase identification [4, 12, 14], reflected in the improved mechanical properties, and reduced electrical and thermal conductivities. The complex atomic atmospheric nature in the high-entropy alloy matrix makes the atomic motion difficult [15, 16]; the activation energy for the substitutional atomic diffusion increases to such a high level that the extremely slow diffusion process even lets the survival of nanocrystals in the cast [17] and annealed [18] microstructure. The synergistic effect of these factors dictates the resulting unpredictable extraordinary properties of these high-entropy alloys. The processing route plays a major role in developing the microstructure in non-traditional multi-principle element high-entropy alloys [19], like traditional single-principle element alloys. The ingot metallurgy route using arc melting was the favorite and effective processing route for the majority of the reported alloys, while the powder metallurgy route proved to be competent in processing the high-entropy alloys. The powder metallurgy processing route was dominated by the mechanical alloying method, which involved a large number of repeated cold welding and fracture cycles, followed by the compaction and sintering process to produce the alloys. Despite being relatively less dense than the ingot metallurgy processed alloys, the powder metallurgy processed alloys typically possess superior mechanical properties from their homogeneous or bimodal microstructure [20, 21]. However, the availability of metallic materials in nanometer size powder form has brought a new perspective in processing traditional [22] and non-traditional [10, 23] alloys avoiding mechanical alloying.

Among the reported studies, the lightweight high-entropy alloys are minimally explored. Earlier studies have shown that aluminum-based high-entropy materials are lightweight and display potential of excellent mechanical properties [10, 24–28]. The developed alloys achieved excellent mechanical properties reported in terms of microhardness at the gigapascal level. All of the research work indicated that, in combination with other elements, copper, silicon, and titanium are the most common alloying elements in developing aluminum-based lightweight high-entropy alloy. Considering our recent successful attempt to develop a lightweight, high-entropy alloy [10], the current work aimed to explore the processing of an equiatomic aluminum-silicon-copper-nickel-titanium high-entropy multicomponent intermetallic alloy using a powder metallurgy route involving the blend-press-sinter in a nitrogen environment. The focus was to study the effect of sonication of micron-nanometer size elemental powders and sintering of sonicated powder compact in a nitrogen environment on the evolution of microstructure and mechanical properties of the developed high-entropy alloy.

2. Materials and methods

2.1. Materials and processing

Materials used in this study to develop an $Al_{24.2}$ $Si_{3.25}Cu_{24.2}Ni_{24.2}Ti_{24.2}$ alloy were high purity elemental aluminum (30 μm particles with 95.5+ % purity), silicon (100 nm particles with 99+ % purity), copper (25 nm particles with 99.8 % purity), nickel (20 nm with 99.9+ % purity) and titanium (40–60 nm with 99.9+ % purity) powders. The aluminum powder was purchased from Alpha Chemicals, USA, and the remaining silicon, copper, nickel, and titanium nanopowders were purchased from the Skyspring Nanomaterials Inc., USA.

The powders were blended together in an equiatomic ratio of 24.2, except the silicon, whose atomic ratio was maintained at 3.25. Blending of the micrometer aluminum particles with the nanometer particles of other elements was done to homogenize the distribution of alloying elements using ultrasonication (model VC-50, Sonics) for 10 min in acetone media in a glass beaker. The acetone media were evaporated from the physically blended alloy suspension for 12 h in an oven at 60 ℃, and the dried alloy powder was subsequently compacted into several cylindrical preforms, with 10 mm diameter and 10 mm height, using a pressure of 450 MPa on a uniaxial hydraulic press. The cylindrical preforms were sintered at 700 ℃ for 90 min in a nitrogen environment using a resistance heating tube furnace (model MTI GSL-1700X, MTI Corporation, USA), followed by the furnace cooling. The blended $Al_{24.2}Si_{3.25}Cu_{24.2}Ni_{24.2}Ti_{24.2}$ alloy also was subjected to thermogravimetric analysis (TGA) up to 1000 ℃ in a nitrogen environment (model SDT Q600, TA Instruments, USA) to understand the potential, if any, the chemical intervention of nitrogen during the sintering process.

2.2. Microstructural characterization

The microstructure of the sintered $Al_{24.2}Si_{3.2}$ $Cu_{24.2}Ni_{24.2}Ti_{24.2}$ alloy was analyzed for the pattern of compositional homogeneity and the distribution pattern of the potential phases developed in the material using a field emission scanning electron microscope equipped with energy dispersive spectroscopy (model Quanta 250 FEG, FEI, Czech Republic). To identify the potentially evolved phases in the sintered non-equilibrium $Al_{24.2}Si_{3.2}Cu_{24.2}Ni_{24.2}Ti_{24.2}$ alloy, a metallurgically prepared sample was subjected to Cu K$_\alpha$ radiation (λ = 1.5418 Å) at a rate of $0.02° \, s^{-1}$, between the diffraction angles of 20° to 100°, in an automated X-ray diffractometer (Bruker-AXS D8 Advance – 40 kV/40 mA). Phases including aluminum, silicon, copper, nickel, titanium, and any other possible intermetallic compounds from these el-
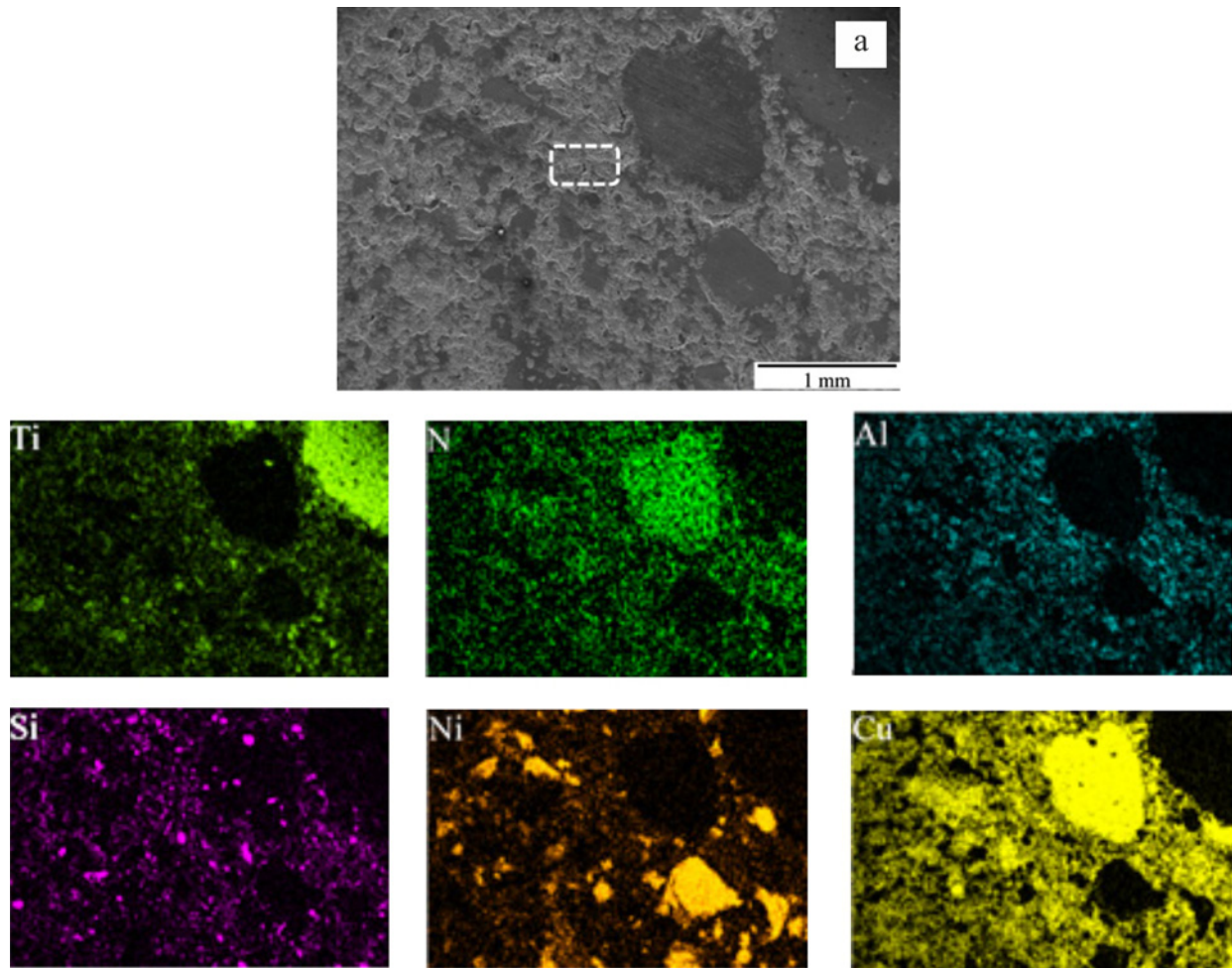
Fig. 1a. FESEM micrograph and associated EDS maps showing elemental distribution pattern in powder processed sintered $Al_{24.2}Si_{3.2}Cu_{24.2}Ni_{24.2}Ti_{24.2}$ alloy at lower magnification.

ements with or without nitrogen were identified by matching Bragg's angle, and the corresponding interplaner spacing formed the diffraction spectrum using the PDXL2 software. X-ray diffraction pattern of unsintered $Al_{24.2}Si_{3.2}Cu_{24.2}Ni_{24.2}Ti_{24.2}$ alloy compact was used as reference. Ambient temperature direct current (DC) conductivity (σ) of the sintered $Al_{24.2}Si_{3.2}Cu_{24.2}Ni_{24.2}Ti_{24.2}$ alloy was measured using a four-in-line probe DC Electrical Conductivity Measuring Instrument (from Scientific Equipment, India) [29] to understand the extent of the presence of possible non-metallic intermetallic in the microstructure. DC electrical conductivity (σ) of unsintered $Al_{24.2}Si_{3.2}Cu_{24.2}Ti_{24.2}Ni_{24.2}$ compact was conducted as reference.

2.3. Mechanical characterization

Microhardness and compressive behavior were studied to understand the mechanical behavior of the sintered $Al_{24.2}Si_{3.2}Cu_{24.2}Ni_{24.2}Ti_{24.2}$ alloy. The Vickers microhardness (HV) value of the sintered $Al_{24.2}Si_{3.2}Cu_{24.2}Ni_{24.2}Ti_{24.2}$ alloy was measured on a metallurgically prepared sample using a Beuhler MMT-3 automatic digital microhardness tester in accordance to the standard ASTM E384-17. 0.5 kgf load and 15 s of dwell time were used in the tests. An ambiance temperature compression test was conducted on the cylindrical sintered samples using an Instron 3367 machine (Instron, USA) according to the standard ASTM E9-09 (2018). The machine cross-head speed was maintained at a rate of $0.050\,mm\,min^{-1}$ during the compression test.

3. Results and discussion

3.1. Macrostructural characteristics

The $Al_{24.2}Si_{3.25}Cu_{24.2}Ni_{24.2}Ti_{24.2}$ alloy was free from any apparent defects in the compact and sintered condition, which was assessed in terms of the presence of bulges or cracks or signs of oxidation. The high-temperature sintering (i.e., 700 °C, higher than
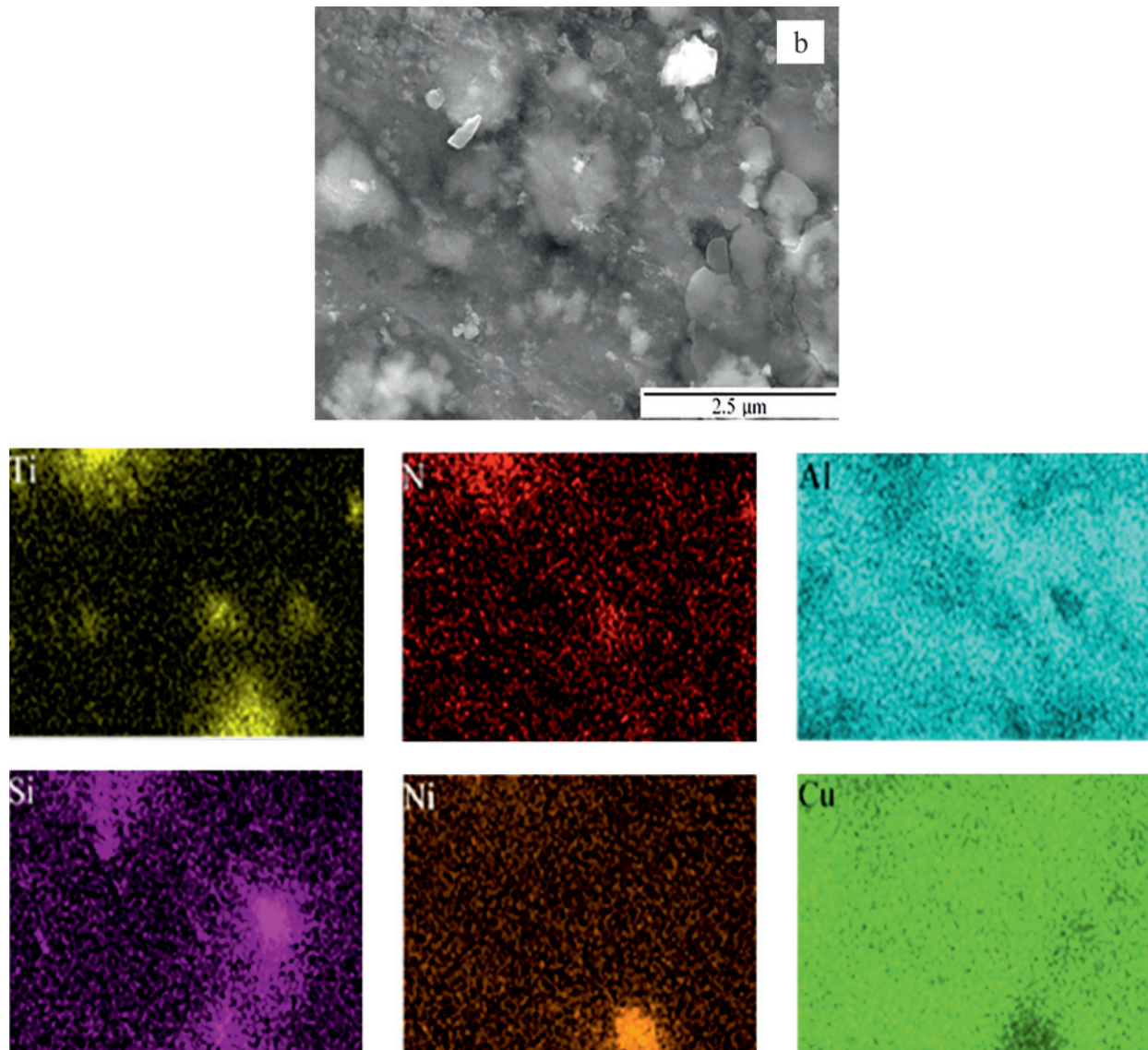
Fig. 1b. FESEM micrograph and associated EDS maps showing elemental distribution pattern in powder processed sintered $Al_{24.2}Si_{3.2}Cu_{24.2}Ni_{24.2}Ti_{24.2}$ alloy at higher magnification of the location in 'white square' shape in Fig. 1a.

the melting temperature of the lowest melting point element, aluminum) did not cause any apparent partial and/or localized melting, which was evident from the smooth and clean surfaces of the sintered samples with unchanged shape and dimension.

3.2. Microstructural characteristics

Results of the microstructural characterization (see Fig. 1) revealed competence of the sonication method in a reasonable homogeneous blending of micrometer aluminum particles with nanometer silicon, copper, nickel, and titanium particles. However, it has to be noted that there is a higher tendency of agglomeration in nanoparticles [30–32]. Hence, the presence of discrete elemental clusters cannot be avoided in the powder metallurgy processing route. Theoret-

ical calculation [33] of the diffusion of elements into aluminum (considering micrometer size particles) has predicted (see Fig. 2a) that silicon, copper, and nickel have reasonable diffusivity at the sintering temperature, while titanium remained almost indiffusible. The mutual solubility of the elements among each other at the sintering temperature used in this study is extremely limited except between copper and nickel [34]. Besides, the distribution pattern of the elements in the compact $Al_{24.2}Si_{3.25}Cu_{24.2}Ni_{24.2}Ti_{24.2}$ alloy microstructure was not in a typical binary-diffusion couple format. Hence, the almost equiatomic amount of multi-elements made the binary inter-diffusion (i.e., elements into aluminum and/or among themselves) difficult [15, 16] and instead led to the formation of intermetallic compounds. Results of the X-ray diffractometry (see Fig. 2b) revealed that the sintering pro-
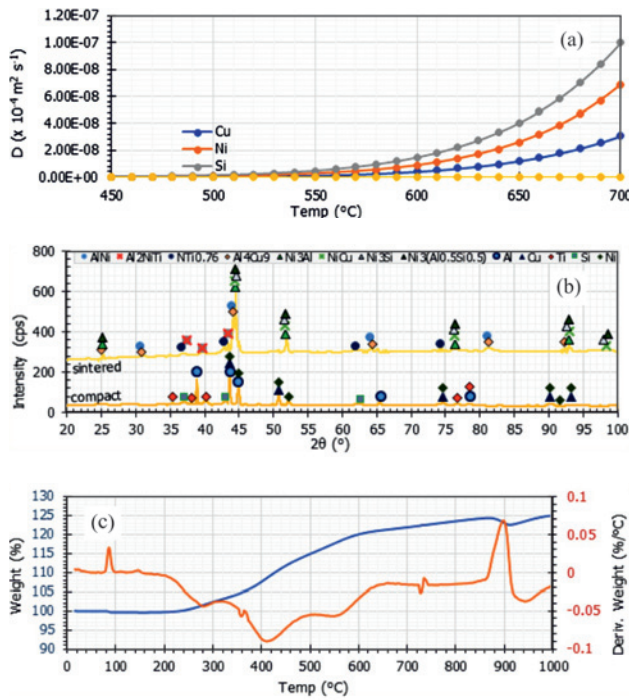
Fig. 2. Graphs showing (a) rate of elemental diffusivity in aluminum, (b) X-ray diffraction spectrum, and (c) thermogravimetric analysis of processed $Al_{24.2}Si_{3.25}Cu_{24.2}Ni_{24.2}Ti_{24.2}$ alloy.

T a b l e 1. Electrical conductivity and mechanical properties of $Al_{24.2}Si_{3.2}Cu_{24.2}Ni_{24.2}Ti_{24.2}$ alloy

Material	Conductivity ($S\,cm^{-1}$)	Hardness (MPa)	Strength (MPa)
Unsintered compact	0.105	–	–
Sintered in N_2	146	797	79
Sintered in Ar [10]	146	1118	310

cess also apparently interferes in the evolution of the microstructure of the $Al_{24.2}Si_{3.25}Cu_{24.2}Ni_{24.2}Ti_{24.2}$ alloy. Nitrogen has substantial solubility in aluminum [35] and titanium [36, 37]. The effect of the nitrogen is evident by the presence of elemental nitrogen in the energy dispersive spectroscopy elemental analysis results (see Fig. 1) and $Ti_{0.76}N$ intermetallic in the X-ray diffractometry spectrum (see Fig. 2b), and also corroborated by the weight gain of the sample in thermogravimetric analysis (TGA) result (see Fig. 2c). Remarkably, the 2θ positions for the X-ray peaks of as-compact and sintered $Al_{24.2}Si_{3.25}Cu_{24.2}Ni_{24.2}Ti_{24.2}$ alloy coincided and misrepresented the identity of the intermetallics in the sintered samples as pure elements. However, the direct current conductivity retention test result of the $Al_{24.2}Si_{3.25}Cu_{24.2}Ni_{24.2}Ti_{24.2}$ alloy samples revealed that the electrically conductive unsintered compact (i.e., $146\,S\,cm^{-1}$) transformed into an almost insulator (i.e., $0.053\,S\,cm^{-1}$) due to sintering, justifying the alteration in microstructure to non-metallic bonded intermetallic phases.

The added elemental particles were well bonded $Al_{24.2}Si_{3.25}Cu_{24.2}Ni_{24.2}Ti_{24.2}$ alloy (see Fig. 3) due to the high-temperature sintering, which was higher than

cess was successful in forming inter-diffusion induced multiple intermetallic compounds and identified most of them as binary in nature. The result was reasonably similar to our previous study [10], where the sintering was done at 600 °C for a much longer time under an inert argon atmosphere (see Table 1).

The presence of nitrogen during the sintering pro-
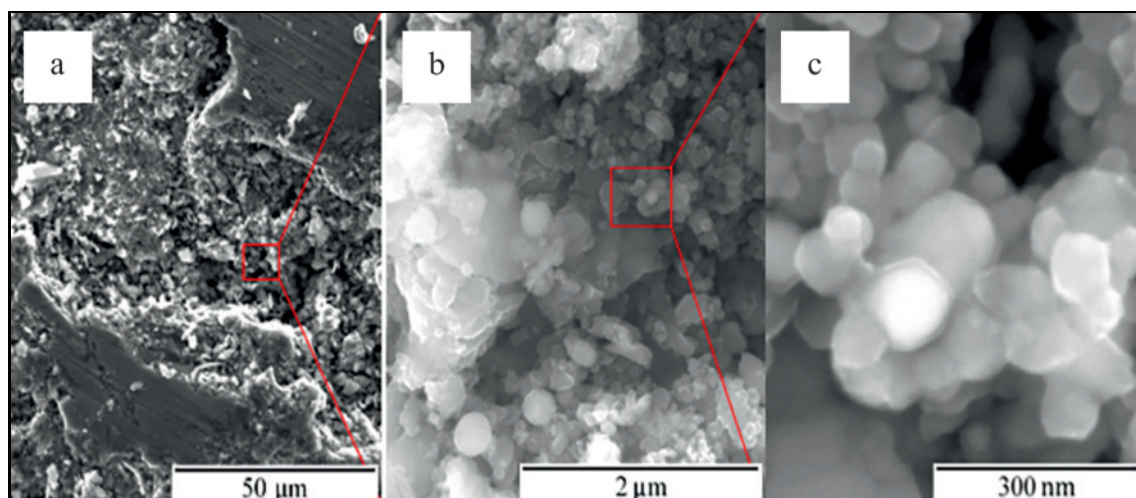
Fig. 3. Field emission scanning electron microscopy showing diffusion assisted bonding among elemental particles in sintered $Al_{24.2}Si_{3.2}Cu_{24.2}Ni_{24.2}Ti_{24.2}$ alloy.
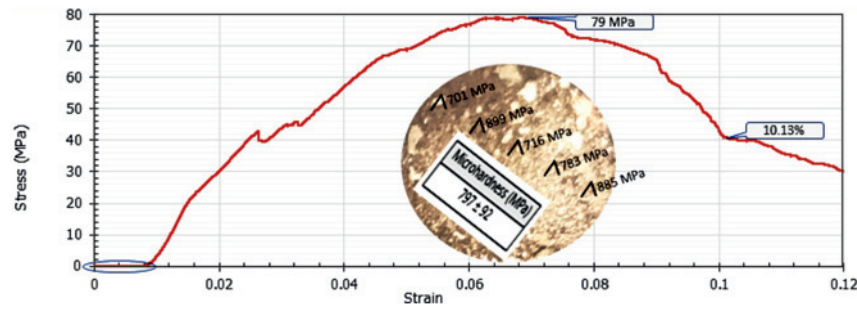
Fig. 4. Graph showing compressive stress-strain behavior of the sintered $Al_{24.2}Si_{3.2}Cu_{24.2}Ni_{24.2}Ti_{24.2}$ alloy. (Inset showing the microhardness values).

the melting point of aluminum and aluminum-silicon eutectic [38]. The bonds between the added particles were indicative of the mutual inter-diffusion, although restricted due to the complex non-equilibrium composition between the elements. The absorption of nitrogen was believed to complicate further the diffusion process and accelerated the formation of the intermetallic compounds layer on metal particles with a possibility of inward growth covering the entire particle considering their initial extremely fine sizes. The likelihood of ternary intermetallic compound formation (one identified in X-ray diffraction) from the binary intermetallic compounds [39, 40] was there in the $Al_{24.2}Si_{3.25}Cu_{24.2}Ni_{24.2}Ti_{24.2}$ alloy in the sintering temperature used in this study.

3.3. Mechanical characteristics

Results of the mechanical characterization (see Fig. 4) revealed a significantly high average value of microhardness (i.e., 797 ± 92 MPa) for the sintered $Al_{24.2}Si_{3.25}Cu_{24.2}Ni_{24.2}Ti_{24.2}$ alloy and could be attributed to the formation of multiple intermetallic compounds. Intermetallic compounds are exceptionally harder than their fundamental basis, even if the elements form a solid solution. Large scatter in the microhardness values (see inset in Fig. 4) was apparently due to the cumulative effect of the relatively scattered cluster of compositional elements (see Fig. 1a) and the porosity (see Fig. 3, part with the highest magnification). It has to be noted that the presence of porosity is typically unavoidable in powder-processed metals [38].

Results of the mechanical characterization also revealed that the compressive stress-strain graph of the sintered $Al_{24.2}Si_{3.25}Cu_{24.2}Ni_{24.2}Ti_{24.2}$ alloy resembles the failure of dense metallic materials. There was a near-linear increment in the stress value indicative of elastic deformation followed by a sharp minor decline for possible plastic deformation. The sintered $Al_{24.2}Si_{3.25}Cu_{24.2}Ni_{24.2}Ti_{24.2}$ alloy experienced a significant strain hardening effect, and the strength value gradually increased to the peak (79 MPa) prior to the

failure with a strain value of 10 %. However, the relatively low value of the compressive strength could have been due to the cumulative effect of the presence of nanopores and/or relatively more minor densification (see Fig. 3) resulting from the presence of nitrogen (absorbed into elements) (see Fig. 1), complex nature of elemental mixture and the duration of the sintering process. The presence of the nanopores around the less diffused particles with intermetallic shells made the inter-particles crack propagation easy, suggested by the chip-off rough polished surface of the sintered $Al_{24.2}Si_{3.25}Cu_{24.2}Ni_{24.2}Ti_{24.2}$ alloy (see Fig. 3). The applied compressive cracked the thin intermetallic surface layer of the particle surfaces and propagated easily with the assistance of nanopores, resulting in fracture more as porous metal. It has to be noted that the values of compressive stress-strain for the same alloy composition sintered for a longer duration in an inert argon atmosphere were relatively higher [10].

4. Conclusions

Non-ferrous $Al_{24.2}Si_{3.25}Cu_{24.2}Ni_{24.2}Ti_{24.2}$ high-entropy alloy was synthesized by blending micrometer and nanometer size elemental particles using a sonication process followed by high-temperature sintering in the nitrogen gas environment. During the sintering process, the elements were dispersed fairly well during blending, absorbed nitrogen defused reasonably, and formed multiple intermetallic elements, including nitride. Despite having a higher microhardness value, the strength was relatively lower due to the presence of nanopores in the microstructure due to the complexity in diffusion and shorter diffusion time.

Acknowledgement

References

[1] B. Cantor, I. T. H. Chang, P. Knight, A. J. B. Vincent, Microstructural development in equiatomic multicomponent alloys, Mater. Sci. Eng. A 375–377 (2004) 213–218. https://doi.org/10.1016/j.msea.2003.10.257

[2] J. W. Yeh, S. K. Chen, J. Y. Gan, S. J. Lin, T. S. Chin, T. T. Shun, C. H. Tsau, S. Y. Chang, Formation of simple crystal structures in Cu-Co-Ni-Cr--Al-Fe-Ti-V alloys with multiprincipal metallic elements, Metal. Mater. Trans. A 35 (2004) 2533–2536. https://doi.org/10.1007/s11661-006-0234-4

[3] S. Ranganathan, Alloyed pleasures: multimetallic cocktails, Curr. Sci. 85 (2003) 1404–1406.

[4] J. W. Yeh, S. K. Chen, S. J. Lin, J. Y. Gan, T. S. Chin, T. T. Shun, C. H. Tsau, S. Y. Chang, Nanostructured high-entropy alloys with multiple principal elements: Novel alloy design concepts and outcomes, Adv. Eng. Mater. 6 (2004) 299–303. https://doi.org/10.1002/adem.200300567

[5] D. B. Miracle, O. N. Senkov, A critical review of high--entropy alloys and related concepts, Acta Mater. 122 (2017) 448–511. https://doi.org/10.1016/j.actamat.2016.08.081

[6] J. M. Torralba, P. Alvaredo, A. G. Junceda, High-entropy alloys fabricated via powder metallurgy – A critical review, Powder Metal. 62 (2019) 84–114. https://doi.org/10.1080/00325899.2019.1584454

[7] R. B. Mane, Y. Rajkumar, B. B. Panigrahi, Sintering mechanism of CoCrFeMnNi high-entropy alloy powders, Powder Metal. 61 (2018) 131–138. https://doi.org/10.1080/00325899.2018.1433268

[8] A. Emamifar, B. Sadeghi, P. Cavaliere, H. Ziaei, Microstructural evolution and mechanical properties of AlCrFeNiCoC high-entropy alloy produced via spark plasma sintering, Powder Metal. 62 (2019) 61–70. https://doi.org/10.1080/00325899.2019.1576389

[9] N. Eißmann, B. Klöden, T. Weißgärber, B. Kieback, High-entropy alloy CoCrFeMnNi produced by powder metallurgy, Powder Metal. 60 (2017) 184–197. https://doi.org/10.1080/00325899.2017.1318480

[10] S. F. Hassan, G. J. Nadhreen, M. A. A. Al-Jeddawi, M. Al-Otaibi, Effect of powder processing on microstructure and mechanical properties of a high--entropy $Al_{24.2}Si_{3.2}Cu_{24.2}Ti_{24.2}Ni_{24.2}$ alloy, Phil. Mag. Let. 100 (2020) 171–180. https://doi.org/10.1080/09500839.2020.1740810

[11] D. B. Miracle, J. D. Miller, O. N. Senkov, C. Woodward, M. D. Uchic, J. Tiley, Exploration and development of high entropy alloys for structural applications, Entropy 16 (2014) 494–525. https://doi.org/10.3390/e16010494

[12] J. W. Yeh, Recent progress in high entropy alloys, Ann. Chim-Sci. Mat. 31 (2006) 633–648. https://doi.org/10.4028/www.scientific.net/AMR.631-632.227

[13] J. Gild, Y. Zhang, T. Harrington, S. Jiang, T. Hu, M. C. Quinn, W. M. Mellor, N. Zhou, K. Vecchio, J. Luo, High-entropy metal diborides: A new class of high-entropy materials and a new type of ultrahigh temperature ceramics, Sci. Rep. 6 (2016) 37946. https://doi.org/10.1038/srep37946

[14] J. W. Yeh, S. Y. Chang, Y. D. Hong, S. K. Chen, S. J. Lin, Anomalous decrease in X-ray diffraction intensities of Cu-Ni-Al-Co-Cr-Fe-Si alloy systems with multiprincipal elements, Mater. Chem. Phys. 103 (2007) 41–46. https://doi.org/10.1016/j.matchemphys.2007.01.003

[15] K. Y. Tsai, M. H. Tsai, J. W. Yeh, Sluggish diffusion in Co-Cr-Fe-Mn-Ni high-entropy alloys, Acta Mater. 61 (2013) 4887–4897. https://doi.org/10.1016/j.actamat.2013.04.058

[16] W. Kucza, J. Dąbrowa, G. Cieślak, K. Berent, T. Kulik, M. Danielewski, Studies of "sluggish diffusion" effect in Co-Cr-Fe-Mn-Ni, Co-Cr-Fe-Ni and Co-Fe-MnNi high entropy alloys; determination of tracer diffusivities by combinatorial approach, J. Alloys Compd. 731 (2018) 920–928. https://doi.org/10.1016/j.jallcom.2017.10.108

[17] C. J. Tong, Y. L. Chen, S. K. Chen, J. W. Yeh, T. T. Shun, C. H. Tsau, S. J. Lin, S. Y. Chang, Microstructure characterization of $Al_xCoCrCuFeNi$ high-entropy alloy system with multiprincipal elements, Metall. Mater. Trans. A 36 (2005) 881–893. https://doi.org/10.1007/s11661-005-0283-0

[18] H. W. Chang, P. K. Huang, J. W. Yeh, A. Davison, C. H. Tsau, C. C. Yang, Influence of substrate bias, deposition temperature and post-deposition annealing on the structure and properties of multiprincipal-component (AlCrMoSiTi)N coatings, Surf. Coat. Technol. 202 (2008) 3360–3366. https://doi.org/10.1016/j.surfcoat.2007.12.014

[19] Y. Zhang, T. T. Zuo, Z. Tang, M. C. Gao, K. A. Dahmen, P. K. Liaw, Z. P. Lu, Microstructures and properties of high-entropy alloys, Prog. Mater. Sci. 61 (2014) 1–93. https://doi.org/10.1016/j.pmatsci.2013.10.001

[20] A. W. Weeber, H. Bakker, H. J. M. Heijligers, G. F. Bastin, Compositional analysis of NiZr powder during amorphization by mechanical alloying, Europhys. Lett. 3 (1987) 1261. http://dx.doi.org/10.1209/0295-5075/3/12/003

[21] S. Varalakshmi, M. Kamaraj, B. S. Murty, Formation and stability of equiatomic and nonequiatomic nanocrystalline CuNiCoZnAlTi high-entropy alloys by mechanical alloying, Metall. Mater. Trans. A 41 (2010) 2703–2709. https://doi.org/10.1007/s11661-010-0344-x

[22] S. F. Hassan, M. T. Islam, S. Nouari, M. M. A. Baig, F. Patel, N. Al-Aqeeli, Extraordinary strengthening of magnesium by the solid-state diffusion of copper in Mg-0.5Cu alloy, JOM 72 (2020) 1597–1606. https://doi.org/10.1007/s11837-020-04023-9

[23] S. F. Hassan, O. Siddiqui, M. F. Ahmed, A. I. Al Nawwah, Development of gradient concentrated single phase fine Mg-Zn particles and effect on the structure and mechanical properties, J. Eng. Mater. Technol. 141 (2018) 021007. https://doi.org/10.1115/1.4041865

[24] K. M. Youssef, A. J. Zaddach, C. Niu, D. L. Irving, C. C. Koch, A novel low-density, high-hardness, high--entropy alloy with close-packed single-phase nanocrystalline structures, Mater. Res. Lett. 3 (2015) 95–99. https://doi.org/10.1080/21663831.2014.985855

[25] Y. Jia, Y. Jia, S. Wu, X. Ma, G. Wang, Novel ultralight-weight complex concentrated alloys with

high strength, Materials 12 (2019) 1136.
https://doi.org/10.3390/ma12071136

[26] P. Chauhan, S. Yebaji, V. N. Nadakuduru, T. Shanmugasundaram, Development of a novel light weight $Al_{35}Cr_{14}Mg_6Ti_{35}V_{10}$ high entropy alloy using mechanical alloying and spark plasma sintering, J. Alloys Compd. 820 (2020) 153367.
https://doi.org/10.1016/j.jallcom.2019.153367

[27] J. M. Sanchez, I. Vicario, J. Albizuri, T. Guraya, J. C. Garcia, Phase prediction, microstructure and high hardness of novel lightweight high entropy alloys, J. Market. Res. 8 (2019) 795–803.
https://doi.org/10.1016/j.jmrt.2018.06.010

[28] K. Tseng, Y. Yang, C. Juan, T. Chin, C. Tsai, J. Yeh, A lightweight high-entropy alloy $Al_{20}Be_{20}Fe_{10}Si_{15}Ti_{35}$, Sci. China Technol. Sci. 61 (2018) 184–188.
https://doi.org/10.1007/s11431-017-9073-0

[29] Instruction Manual of four-in-line probe DC Electrical Conductivity Measurement Instrument, Scientific Equipments and Services, Roorkee, India.

[30] G. N. Hassold, E. A. Holm, D. J. Srolovitz, Effects of particle size on inhibited grain growth,Scripta Metallurgica et Materialia 24 (1990) 101–106.
http://dx.doi.org/10.1016/0956-716X(90)90574-Z

[31] J. P. Wilcoxon, B. L. Abrams, Synthesis, structure and properties of metal nanoclusters, Chem. Soc. Rev. 35 (2006) 1162–1194.
https://doi.org/10.1039/B517312B

[32] J. Hassinen, Noble Metal Nanoparticles and Clusters, [PhD Dissertation], Espoo, Aalto University 2016.

[33] G. Neumann, C. Tuijn, Self-Diffusion and Impurity Diffusion in Pure Metals: Handbook of Experimental Data, Elsevier, Oxford, UK, 2009.

[34] T. Lyman, Metal Handbook, Vol. 8, 8th Edition, American Society for Metals, Metals Park, Ohio, 1973.

[35] T. Schubert, T. Pieczonka, S. Baunack, B. Kieback, The influence of the atmosphere and impurities on the sintering behaviour of aluminium, Proceedings of Euro PM 2005: Powder Metallurgy Congress and Exhibition, Vol. 1, Prague, 2005, pp. 3–8.

[36] H. Conrad, Effect of interstitial solutes on the strength and ductility of titanium, Prog. Mater. Sci. 26 (1981) 123–403.
https://doi.org/10.1016/0079-6425(81)90001-3

[37] H. A. Wriedt, J. L. Murray, The N-Ti (Nitrogen-Titanium) system, Bulletin of Alloy Phase Diagrams 8 (1987) 378–388.
https://doi.org/10.1007/BF02869274

[38] S. Kalpakjian, S. R. Schmid, Manufacturing Processes for Engineering Materials, 5th Edition, Pearson Prentice Hall, Singapore, 2008. ISBN-13: 978-0134290553

[39] K. J. Lee, P. Nash, The Al-Ni-Ti system (Aluminum--Nickel-Titanium), J. Phase Equil. 12 (1991) 551–562.
https://doi.org/10.1007/BF02645068

[40] G. Effenberg, S. Ilyenko, Ternary Alloy Systems: Phase Diagrams, Crystallographic and Thermodynamic Data Light Metal Systems, Part 2, Landolt--Börnstein – Group IV Physical Chemistry, Vol. 11A2, 2005. ISBN: 978-3-540-23118-9